J Geod (2009) 83:1083–1094
DOI 10.1007/s00190-009-0326-1

ORIGINAL ARTICLE

High-rate GPS clock corrections from CODE: support of 1 Hz applications

H. Bock · R. Dach · A. Jäggi · G. Beutler

Received: 10 March 2009 / Accepted: 28 May 2009 / Published online: 13 June 2009

Abstract GPS zero-difference applications with a sampling rate up to 1 Hz require corresponding high-rate GPS clock corrections. The determination of the clock corrections in a full network solution is a time-consuming task. The Center for Orbit Determination in Europe (CODE) has developed an efficient algorithm based on epoch-differenced phase observations, which allows to generate high-rate clock corrections within reasonably short time (<2 h) and with sufficient accuracy (on the same level as the CODE rapid or final clock corrections, respectively). The clock determination procedure at CODE and the new algorithm is described in detail. It is shown that the simplifications to speed up the processing are not causing a significant loss of accuracy for the clock corrections. The high-rate clock corrections have in essence the same quality as clock corrections determined in a full network solution. In order to support 1 Hz applications 1-s clock corrections would be needed. The computation time, even for the efficient algorithm, is not negligible, however. Therefore, we studied whether a reduced sampling is sufficient for the GPS satellite clock corrections to reach the same or only slightly inferior level of accuracy as for the full 1-s clock correction set. We show that high-rate satellite clock corrections with a spacing of 5 s may be linearly interpolated resulting in less than 2% degradation of accuracy.

Keywords High-rate · GPS clock corrections · IGS · 1 Hz

H. Bock (✉) · R. Dach · A. Jäggi · G. Beutler
Astronomical Institute, University of Bern,
Sidlerstr. 5, 3012 Bern, Switzerland
e-mail: heike.bock@aiub.unibe.ch

1 Introduction and motivation

The knowledge of precise satellite clock corrections is essential for Precise Point Positioning (PPP, Zumberge et al. 1997) applications using the Global Positioning System (GPS). Kinematic positioning of moving objects, in particular precise orbit determination (POD) for low Earth orbiting (LEO) satellites like the CHAMP (Reigber et al. 2002), the two GRACE (Tapley et al. 2004), or the recently launched GOCE (Drinkwater et al. 2006) satellite, are important applications of PPP. The accuracy of these POD applications is among other things dependent on the sampling of the GPS clock corrections. Montenbruck et al. (2005) showed that linearly interpolated 5-min GPS clock corrections are not sufficient to achieve highly accurate (few cm-level) POD results for LEO satellites using PPP approaches with 30-s sampled GPS data. GPS satellite clock corrections with the same sampling as the observations (i.e., 30 s) are necessary.

The International GNSS (Global Navigation Satellite Systems) Service (IGS) (Dow et al. 2009) has provided a product for precise GPS satellite clock corrections for quite some time. The clock corrections are, however, only available with a sampling of 5 min over years. The processing time for a solution with a higher sampling rate increases roughly proportional to the number of additional epochs involved. Therefore, it took a very long time until four analysis centers were able to deliver 30-s GPS clock corrections for the entire GPS constellation (at least three contributions are needed to provide a reliable combined product). Since GPS week 1406 (December 17, 2006) a combined final clock product is available with a sampling of 30 s (Gendt 2006). Three to four IGS analysis centers, namely CODE (Center for Orbit Determination in Europe), Bern, Switzerland, JPL (Jet Propulsion Laboratory), Pasadena, California, USA (until GPS week 1441), MIT (Massachusetts Institute of

Technology), Cambridge, Massachusetts, USA, and NRCan (National Resources Canada), Ottawa, Canada are the contributors.

CODE, located at the Astronomical Institute of the University of Bern (AIUB), Switzerland, a joint venture of AIUB, the Federal Office of Topography, swisstopo, Wabern, Switzerland, the Federal Agency for Cartography and Geodesy (BKG), Frankfurt a. Main, Germany, and the Institut für Astronomische und Physikalische Geodäsie, Technische Universität München, Germany, started to generate 5-min GPS clock corrections in September 1995 (Springer 2000) and 30-s GPS clock corrections in 1999 (Bock et al. 2000). An efficient approach for generating high-rate GPS clock corrections was developed to support the initial activities in the field of POD for LEO satellites (Bock et al. 2002; Bock 2004). This approach is much less time-consuming than a full 30-s network solution. The basic idea has already been to use epoch-differenced phase observations for the determination of the high-rate clock corrections. It was further developed, improved, and implemented in the daily GPS clock correction determination at CODE. Since GPS week 1265 (April 4, 2004), these high-rate GPS clock corrections are delivered to the IGS as part of the CODE final clock product as well as the CODE rapid clock product (Hugentobler 2004). These official final CODE clock products and high-rate clocks partly generated for earlier periods were used for LEO POD activities (Jäggi et al. 2006; Jäggi 2007; Jäggi et al. 2007) at AIUB. The CODE 30-s GPS clock corrections are also used in other GPS processing software packages for LEO POD (e.g., Montenbruck et al. 2005; Kroes 2006; Van Helleputte and Visser 2008; Hwang et al. 2008).

The AIUB is member of the European GOCE Gravity-Consortium (EGG-C) and thus part of the GOCE High-level Processing Facility (HPF, Koop et al. 2006). Within the HPF, the institute is responsible for the generation of the Precise Science Orbit (PSO) (Bock et al. 2007) for the GOCE satellite. In order to support the POD for GOCE delivering 1 Hz GPS tracking data, 5-s high-rate GPS clock corrections are generated at AIUB within the framework of the HPF. The approach followed for the generation of these 5-s GPS clock corrections is based on that used for the CODE 30-s GPS clock corrections. Since the start of GPS week 1478 (May 3, 2008) CODE is producing 5-s GPS clock corrections even as the CODE final clock product (Schaer and Dach 2008). In order to use these 5-s clock corrections for 1 Hz applications they have to be interpolated by the users.

The generation of high-rate GPS clock corrections is an integrated part of the GPS clock correction determination procedure at CODE. The preceding low-rate (i.e., 5 min) clock correction determination is a mandatory prerequisite for the efficient high-rate clock interpolation (EHRI) approach. Therefore, an overview and a description of the complete GPS satellite and station clock correction determination procedure at CODE is given in Sect. 2. Section 3 presents the efficient algorithm in detail for the EHRI, which is used for the high-rate (30 and 5 s) clock generation, and addresses the evaluation of the simplifications made within our algorithm. In Sect. 4 the quality of the step-wise generated clock corrections is validated and in Sect. 5 the quality of the linear clock correction interpolation from 5 to 1 s is assessed. Section 6 addresses an important application of the high-rate clock corrections and Sect. 7 contains the summary and the conclusion.

2 Clock correction determination procedure at CODE

The GPS clock correction determination procedure is part of a large number of daily processes running at CODE (Dach et al. 2009). All products delivered to the IGS are computed using the Bernese GPS Software Version 5.1 (development version) (Dach et al. 2007). The parameter estimation procedures within the software package are all based on a classical least squares adjustment. The underlying physical models for the data processing are based to the extent possible on the most recent IERS conventions (McCarthy and Petit 2004). The current CODE processing standards may be found at http://www.aiub.unibe.ch/download/CODE/CODE.ACN.

The GNSS orbit estimation procedure is the core of the CODE analyses and the solution is derived with a global double-difference network solution. The double-difference technique is used because the satellite and receiver clock corrections are not required for many GNSS applications. The double-difference processing considerably reduces the number of parameters to be estimated. The remaining parameters are GNSS orbit parameters, Earth Rotation Parameters (ERPs), ionosphere parameters, coordinates, and troposphere parameters for each station involved. The orbit estimation part includes GLONASS (GLObal NAvigation Satellite System, the Russian counterpart of GPS) satellite orbits.

In order to determine clock corrections we have to set up a zero-difference processing. The parameters already estimated in the preceding orbit estimation procedure are fixed to their previously estimated values and build the reference frame for the clock corrections.

GLONASS is not yet included into the clock correction procedure and therefore CODE currently delivers GPS-only clock products to the IGS. Two different products are delivered, namely the rapid and the final product. The two products differ in precision (standard deviation of the clock corrections with respect to the IGS combination: 20–30 ps for rapid, about 15 ps for final), sampling (30 s for rapid, 5 s for final), and latency of delivery to the IGS (1 day for rapid, 10–13 days for final). The clock estimation procedure is performed in the following steps:

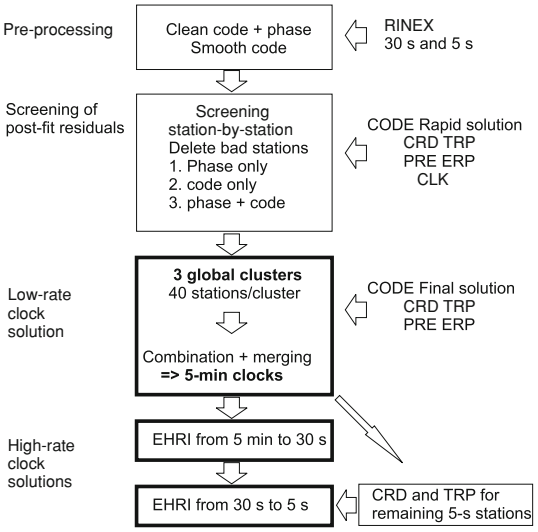

Fig. 1 Flow chart for final clock generation at CODE (CRD: coordinates, TRP: troposphere parameters, ERP: Earth Rotation Parameters, PRE: precise GNSS satellite orbits, CLK: GNSS satellite and station clock corrections)

- Pre-processing of the GPS tracking data
- Screening of post-fit observation residuals
  - Rapid: in small regional networks
  - Final: PPP, rapid orbit and clock solution is used
- Low-rate clock solution (5-min sampling)
- High-rate clock solutions (see Sect. 3)
  - EHRI, 30-s sampling
  - Only final: EHRI, 5-s sampling.

Figure 1 shows the flow chart for the complete (low- and high-rate) final clock generation at CODE. Data from a global network (IGS network) of at maximum 90 stations for the rapid and 120 stations for the final clock analysis is processed. The stations are selected according to the receiver clock type. Stations with hydrogen masers (e.g., ALGO, Algonquin Park, Ontario, Canada) and stations operated by time laboratories (e.g., PTBB, Braunschweig, Germany and WAB2, Wabern, Switzerland) are selected with the highest priority.

The IGS high-rate (1 Hz) network is used for the 5-s clock correction determination in the final clock procedure. The availability of such high-rate data is a prerequisite for the determination of clock corrections with a sampling higher than 30 s. The number of stations delivering high-rate data is also important because a minimum number of globally distributed stations is needed to get a reasonable clock correction solution. Figure 2 shows the development over the years of the number of stations delivered to the global IGS data center CDDIS (Crustal Dynamics Data Information Service, Greenbelt, Maryland, USA). The number increased from initially

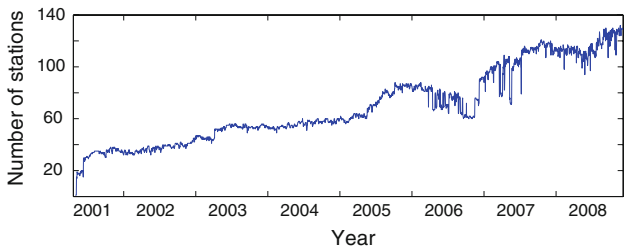

Fig. 2 Number of IGS 1-Hz stations available at CDDIS

about 20 stations to about 130 stations towards the end of 2008. Though in the meantime the number of stations is large enough for a good coverage and a reliable clock correction determination, completeness of these high-rate data is still a problem (see http://www.ngs.noaa.gov/IGSWorkshop2008/docs/CODE_high_rate_clocks.pdf). In addition, the IGS standards are not followed by all the stations, in particular the equipment is not known sufficiently well due to missing station log files and incomplete RINEX header information.

The 1-Hz tracking data are available at two of the four global IGS data centers (Noll et al. 2009), namely at CDDIS and at KASI (Korea Astronomy and Space Science Institute, Seoul, Korea). Part of the data is also available at the global data center of IGN (Institut Géographique National, Paris, France) and at the regional data center at BKG. About 100 stations are used for the high-rate clock correction determination. Figure 3 shows the stations used for the 5-s clock correction determination on day 326/2008 (November 21, 2008) as a typical situation by the end of 2008. The stations have a good global distribution, which is essential for a reliable and complete clock correction determination, where all satellites have to be observed by at least three stations for all observation epochs.

2.1 Pre-processing

The pre-processing of the GNSS data is based on RINEX (Gurtner 1994) files. Each RINEX file is processed separately

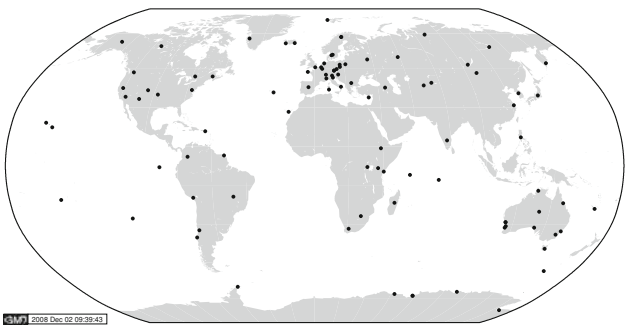

Fig. 3 Distribution of IGS 1-Hz stations used for the 5-s high-rate clock correction determination on day 326/2008 (November 21, 2008)

and no additional information is required. Three linear combinations (LCs) of the original L1 and L2 observations are formed to screen the data:

- Melbourne-Wübbena: This LC is screened for outliers and cycle slips.
- Geometry-free (only when a cycle slip is found in the Melbourne-Wübbena LC): The size of the cycle slips is determined to connect the code observations later in the code smoothing process. For the phase observations a new ambiguity parameter is set up.
- Ionosphere-free: The difference between the ionosphere-free LC from code and phase measurements is screened for outliers.

The consistency of all four observation types (code and carrier phase on both frequencies) is checked. In addition, the code observations are smoothed using carrier phase measurements (Springer 2000).

2.2 Screening of post-fit residuals

2.2.1 Rapid analysis

The stations are grouped into 12 regional clusters. The GNSS orbits, ERPs, station coordinates, and troposphere parameters are taken from the CODE rapid 3-days (Beutler et al. 1996) double-difference solution. If a station was not part of this double-difference solution, the corresponding station-specific parameters (station coordinates and troposphere parameters) are estimated in the cluster solution. The clock corrections (satellites and stations) and the initial phase ambiguities are estimated independently for each cluster. The residuals are checked for outliers and the corresponding observations are marked. In a second iteration step, a station may appear in more than one cluster to guarantee a minimum redundancy for each observation to detect the remaining outliers.

2.2.2 Final analysis

For the final analysis screening is performed station-by-station in a PPP mode. The GNSS orbits, ERPs, station coordinates, and troposphere parameters are again taken from the CODE rapid double-difference solution and additional parameters are estimated for stations not included in the rapid solution.

Code and phase observations are processed separately in a first step. After checking the residuals for outliers and flagging the corresponding observations as unusable a consistency check is made by using both measurement types in a common analysis.

2.3 Low-rate clock solution 5-min sampling

Three global clusters are built up with at maximum 30 stations each for the rapid and at maximum 40 stations for the final analysis.

For this clock solution the GNSS orbits, ERPs, station coordinates, and troposphere parameters are taken from the corresponding double-difference solution (CODE rapid results for the determination of the rapid clock corrections and CODE final results for the determination of the final clock corrections). If a station was not part of this solution the coordinates and troposphere parameter are set up as unknown parameters for these stations.

The large number of clock parameters (one per GPS satellite and receiver for each epoch) are pre-eliminated epoch-by-epoch from the normal equation (NEQ) system and recovered at the end in a back-substitution step.

The cluster solutions are combined by estimating epoch-wise clock offsets between the individual clusters and referring therewith all clocks to the same reference clock. Though it is not important for the quality of the clock solution which clock is selected as reference clock, a sophisticated procedure is set up to find the most stable and "best behaving" (linear) clock as reference clock: In separate parameter estimation steps each receiver clock is used once as reference clock and the solution is aligned to this reference clock candidate. All clock corrections are then represented by first-order polynomials and the mean RMS is computed and stored. The candidate clock yielding the smallest mean fit RMS and having a complete set of clock values available is then selected as reference clock. A linear reference clock gives the possibility to better inter- and extrapolate the clock solutions. In addition, the selection of the best clock as reference is also used as control of the clock solution (receiver clocks with problems are detected). In the year 2008, e.g., these reference clocks always have been hydrogen maser clocks (24 different stations) and the two master clock stations in USA at USNO (U.S. Naval Observatory, Washington, D.C.) with 75 days and at AMC2 (Alternate Master Clock, Colorado Springs, Colorado) with 61 days have been selected most.

To keep the efficiency of the following EHRI algorithm for the 30- and 5-s clock determination coordinates and troposphere parameters need to be known for all stations. Not all 5-s stations are included in the full zero-difference network solution and therefore these parameters are computed for all remaining 5-s stations.

3 Algorithm for the EHRI 30- and 5-s sampling

Starting with the precise 5-min clock corrections based on a full zero-difference network solution the 30-s clock corrections are determined using the EHRI algorithm. For the

CODE final clock solution the EHRI algorithm is then used in addition for the determination of the 5-s clock corrections.

To keep the efficiency of the EHRI algorithm GNSS satellite orbits, ERPs, station coordinates, and troposphere parameters have to be available—from the double-difference processing of the global permanent IGS network or the low-rate clock generation procedure (Sect. 2.3)—as well as low-rate (5-min) satellite and receiver clock corrections (Sect. 2). All this information is used for the densification to high-rate clock corrections using the EHRI approach. The procedure consists of the following steps:

- clock synchronization,
- clock estimation based on code observations,
- clock-difference estimation based on phase-difference observations,
- clock combination,
- reference clock selection.

The algorithm is used for the 30- and 5-s high-rate clock correction densification. For sake of simplicity we will explain the algorithm only for the generation of the 30-s clock corrections. Parameter estimation is always based on the method of least squares.

3.1 Clock estimation and receiver clock synchronization using code measurements

The receiver clocks have to be synchronized with GPS system time (within 1μ s) so that the error in the geometrical distance between receiver and satellite induced by the receiver clock error is below 1 mm. The synchronization is done using the code measurements. The receiver and satellite clock corrections are estimated separately for each epoch.

We start with the standard GPS code observation equation expressed in meters (somewhat simplified and without error term):

$$p^j_{fk}(t_i) = \rho^j_k(t_i) - c \cdot \delta^j(t_i) + c \cdot \delta_k(t_i) + \rho^j_{fk,\mathrm{iono}}(t_i) + \rho^j_{k,\mathrm{trop}}(t_i) + c \cdot b^j, \quad (1)$$

where

p^j_{fk}	is the observed code pseudorange,
ρ^j_k	is the slant distance,
δ^j	is the satellite clock correction,
δ_k	is the receiver clock correction,
$\rho^j_{fk,\mathrm{iono}}$	is the ionospheric refraction,
$\rho^j_{k,\mathrm{trop}}$	is the tropospheric refraction,
b^j	is the differential code bias (DCB), and
c	is the speed of light.

The subscripts k refer to receivers, f specifies the frequency, the superscript j refers to satellites; t_i is the epoch of the measurement.

Precise GPS orbits, ERPs, and station coordinates (geometrical part), troposphere parameters, and DCBs[1] are used as known from the previous 5-min clock solution. The following observation equation results:

$$P^j_{fk}(t_i) = -c \cdot \delta^j(t_i) + c \cdot \delta_k(t_i) + \rho^j_{fk,\mathrm{iono}}(t_i). \quad (2)$$

If we form the ionosphere-free LC CP^j_k of P^j_{1k} and P^j_{2k}, we are left with the satellite and receiver clock corrections only:

$$CP^j_k(t_i) = -c \cdot \delta^j(t_i) + c \cdot \delta_k(t_i). \quad (3)$$

The NEQ system is set up separately for each epoch based on observation equations of this type for all satellites and receivers involved. In order to avoid the NEQ system to become singular, a zero mean condition is set up for all satellite clock corrections involved. The epoch-wise estimation of the clock correction parameters is efficient due to the small number of observations (≈100 stations with 10 satellites in view gives 1,000 observations per epoch) and number of parameters (≈100 receiver +32 satellite clock corrections result in 132 clock parameters to be estimated) compared to a full one-day 30-s network solution with 2,880 epochs.

A data screening step is included in the clock determination procedure. Due to the large amount of data contributing to one parameter, the receiver and satellite clock correction estimations are very robust and the data may be cleaned iteratively. The residuals of the observations are checked and, if the absolute value of a residual exceeds a user-specified value, the observation is marked and excluded in the subsequent iteration steps.

The synchronization with GPS time is achieved by using the estimated receiver and satellite clock corrections derived from the code measurements as a priori values for the phase analysis. In the phase analysis (see Sect. 3.2) the corrections with respect to the clock corrections resulting from the code analysis are estimated.

3.2 Clock-difference estimation using phase-difference observations

The phase measurements are the primary observations for the generation of the high-rate clock corrections.

In analogy to the code processing, the phase observation equation expressed in meters (somewhat simplified and without error term) reads as

[1] DCBs are necessary if at least one of the receivers is tracking the code measurements only on the C/A-code and not on the P-code (Schaer 1999).

$$\phi^j_{fk}(t_i) = \rho^j_k(t_i) - c \cdot \delta^j(t_i) + c \cdot \delta_k(t_i) - \rho^j_{fk,\text{iono}}(t_i) + \rho^j_{k,\text{trop}}(t_i) + \lambda_f \cdot N^j_k, \quad (4)$$

where

ϕ^j_{fk} is the observed phase,
λ_f is the wavelength of frequency f, and
N^j_k is the ambiguity.

Compared to the code observation equation (Eq. 1) we have the ambiguity term $\lambda_f \cdot N^j_k$, no DCBs and the opposite sign for the ionospheric refraction. In order to eliminate the ambiguity term from the observation equation differences of phase measurements referring to subsequent epochs are generated:

$$\Delta\phi^j_{fk}(t_{i+1,i}) = \phi^j_{fk}(t_{i+1}) - \phi^j_{fk}(t_i) \quad (5)$$

Otherwise, the same procedure is applied as in the case of code (Eqs. 2 and 3). The resulting phase observation equation for the ionosphere-free LC $\Delta C\phi^j_k$ reads as

$$\Delta C\phi^j_k(t_{i+1,i}) = -c \cdot \Delta\delta^j(t_{i+1,i}) + c \cdot \Delta\delta_k(t_{i+1,i}). \quad (6)$$

The differences of the epoch-wise estimated code satellite and receiver clock corrections are used as a priori values for the phase-difference processing. Therefore, only the corrections to the a priori clock differences are estimated. They are expected to be small. In case of any inconsistency between code and phase measurements (e.g., millisecond jumps, Dach et al. 2006), the corresponding phase measurements are removed. The NEQ system is regularized using the zero mean condition of all satellite clock corrections involved. Data screening of the phase-difference observations is performed in a similar way as for the code observations.

Phase-difference measurements between subsequent observation epochs are correlated as long as they are "connected" by at least one ambiguity term. Though it is not correct from a statistical point of view these correlations are neglected in our analysis. The efficiency of this approach is based on this simplification. In Sect. 3.4 we will show that these simplifications are allowed over short time intervals of 5 min without losing precision for the clock estimates.

From the variance-covariance matrices of each epoch-difference we get $\sigma_{\Delta\delta^j(t_{i+1,i})}$ for each satellite j and $\sigma_{\Delta\delta_k(t_{i+1,i})}$ for each receiver k. These values are used in the following algorithm providing the high-rate clock corrections for both, satellites and receivers.

3.3 Clock combination

In order to get clock corrections from the clock-differences they have to be put in relation to absolute clock readings, which may be obtained either from the code measurements (Sect. 3.1) or from an external high accuracy time series of clock corrections (e.g., 5-min clock solution). This is done by a clock combination procedure, separately for each individual satellite and receiver clock. For the sake of simplicity we explain the procedure, without an index, for a particular receiver or a particular satellite.

Precise clock corrections with a lower sampling than that of the high-rate data are needed by the combination algorithm. In our case, precise clock corrections with 5-min sampling from the CODE rapid or final clock processing are used. In order to get "absolute" clock corrections from the phase clock-differences, we interpolate the series of known fixed clock corrections with these clock-differences.

A new observation equation system is set up with the phase clock-differences $\Delta\tilde{\delta}(t_{i+1,i})$, $i = 1, \ldots, n-1$ (n is the number of epochs) from the previous step as pseudo-observations. The known clock corrections $\tilde{\delta}_{fix}$ are now introduced as pseudo-observations. They are available at the epochs of the clock set with the 5-min resolution.

The new observation equations are

$$\begin{array}{rrrl}
\delta(t_1) & & & = \tilde{\delta}_{fix}(t_1) \\
-\delta(t_1) + \delta(t_2) & & & = \Delta\tilde{\delta}(t_{2,1}) \\
-\delta(t_2) & + \delta(t_3) & & = \Delta\tilde{\delta}(t_{3,2}) \\
 & \cdots & & \cdots \\
-\delta(t_{i-1}) & + \delta(t_i) & & = \Delta\tilde{\delta}(t_{i,i-1}) \\
 & \delta(t_i) & & = \tilde{\delta}_{fix}(t_i) \\
 & -\delta(t_i) & + \delta(t_{i+1}) & = \Delta\tilde{\delta}(t_{i+1,i}) \\
 & \cdots & & \cdots \\
 & -\delta(t_{n-1}) & + \delta(t_n) & = \Delta\tilde{\delta}(t_{n,n-1}) \\
 & & \delta(t_n) & = \tilde{\delta}_{fix}(t_n)
\end{array} \quad (7)$$

The correlations between the epoch-difference solutions are again neglected and the weight matrix of dimension $d = (n-1) + n_{fix} \times (n-1) + n_{fix}$ (n_{fix}, number of epochs of the lower sampled clock set) is diagonal. The weights for the pseudo-observations $\Delta\tilde{\delta}(t_{i+1,i})$ are taken from the a posteriori RMS values of the previous epoch-difference solutions.

$$p_{\Delta\delta(t_{i+1,i})} = p_{i,i+1} = \frac{\sigma_0^2}{\sigma^2_{\Delta\delta(t_{i+1,i})}}, \quad i = 1, \ldots, n \quad (8)$$

with σ_0 as sigma of unit weight. In order to realize the fixing on the known clock correction values the pseudo-observations $\tilde{\delta}_{fix}(t_i)$ are heavily constrained

$$p_{fix} >> p_{i,i+1}, \quad i = 1, \ldots, n-1. \quad (9)$$

Due to the simple structure of the design and the weight matrix the NEQ matrix is sparse; it is a tridiagonal symmetric matrix. The elements of $\mathbf{N}$ for $i = 1, \ldots, n$ are

$$N_{i,i} = \begin{cases} p_{fix} + p_{i,i+1}; & i = 1 \\ p_{fix} + p_{i-1,i} + p_{i,i+1}; & i = i_{fix} \\ p_{i-1,i} + p_{i,i+1}; & i \neq i_{fix} \\ p_{fix} + p_{i-1,i}; & i = n \end{cases} \quad (10)$$

and

$$N_{i,i+1} = -p_{i,i+1}; \quad i = 1, \ldots, n-1 \tag{11}$$

An efficient solution algorithm of tridiagonal equation systems (based on a Lower-Upper decomposition) may be found in Press et al. (1996).

3.4 The impact of the simplified approach

In order to study the impact of neglecting the correlations of the phase observations of subsequent epochs and the correlations between the epoch-difference solutions, we generate a set of 30-s GPS satellite clock corrections (2 h) in a full network solution based on zero-difference observations, where the correlations are automatically taken into account correctly. This clock correction set is re-sampled to 15 and 5 min, respectively. These two sets are used as input for two new 30-s clock generations based on the EHRI algorithm described in Sects. 3.1–3.3. The computation time for the full network solution is (on a multi-node Linux system with 2.4 GHz CPU processors, only the step described in Sect. 2.3) about 10 min and for the EHRI solutions about 1 min, which indicates very clearly the efficiency of the EHRI approach. The resulting clock correction sets are compared to the original 30-s clock correction set to evaluate the impact of the neglected correlations on the resulting clock combination. Figure 4 shows these comparisons for three satellites as representative examples.

The clock solutions based on 15-min clock corrections and 5-min clock corrections, using the phase-differences for interpolation, differ by up to 30 and 10 ps, respectively, from the full network clock solution.

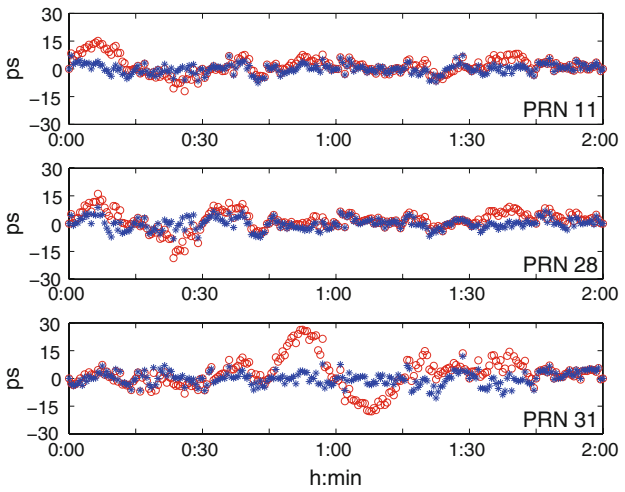

Fig. 4 Clock correction differences with respect to 30-s clock corrections from full network solution; red: 30-s clock corrections densified from 15 min, RMS PRN11: 4.9 ps, PRN28: 5.3 ps, PRN31: 8.7 ps, blue: 30-s clock corrections densified from 5 min, RMS PRN11: 2.7 ps, PRN28: 3.0 ps, PRN31: 3.6 ps

The differences in the clock solutions are a result of ignoring the correlations at the phase-difference observations and between the epoch-difference solutions. The interpolation over 15 min is already critical with RMS values of the differences up to 9 ps. The RMS values for the clock solution, where the phase-differences are used to interpolate 5-min clock corrections, are well below 5 ps (≙1.5 mm). This may be accepted in view of the noise of the phase measurements (3 mm for ionosphere-free LC).

4 Validation of high-rate clock corrections

The first part of the validation (Sect. 4.1) uses the Allan variances of the clock corrections to check whether the step-wise clock determination from 5 min to 30 s and then from 30 to 5 s has an impact on the quality of the clock corrections.

In the second part of the validation, a kinematic PPP for terrestrial stations using the 30-s satellite clock corrections, resampled to 5 min, is performed. Ten different solutions are computed, by shifting the observation epochs by 30 s in subsequent solutions.

4.1 Allan variance studies

Figure 5 shows the Allan deviations (Allan 1987) of three stations

- CAS1: Casey, Antarctica, running on the internal receiver clock,
- MAS1: Maspalomas, Spain, driven by an external Cesium clock, and
- ALGO: Algonquin, Canada, driven by an external hydrogen maser.

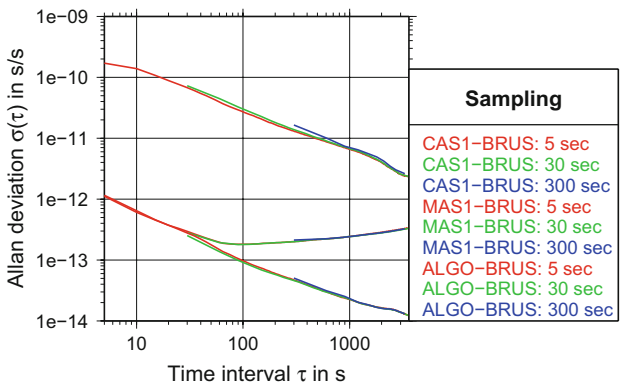

Fig. 5 Allan deviations for the receiver clocks at Casey (CAS1, Antarctica), Maspalomas (MAS1, Spain), and Algonquin (ALGO, Canada) with respect to the reference clock of Brussels (BRUS, Belgium) obtained from the different densification levels with 5 min, 30, and 5 s for day 326 of year 2008

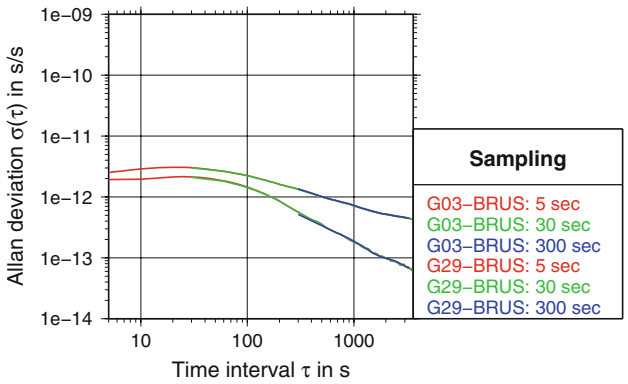

Fig. 6 Allan deviations for the satellite clocks G03 and G29 with respect to the terrestrial reference clock of Brussels (BRUS, Belgium) obtained from the different densification levels with 5 min, 30, and 5 s for day 326 of year 2008

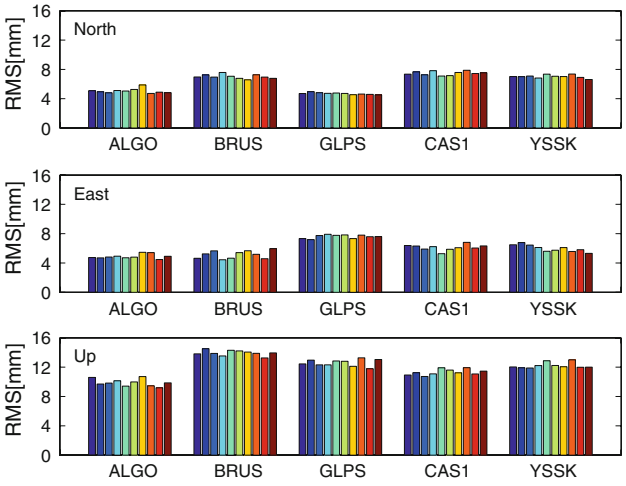

Fig. 7 RMS [mm] of the variations between static and kinematic positions for the nominal 5-min solution (most left bar) and the nine shifted solutions; ALGO: Algonquin Park, Ontario, Canada, BRUS: Brussels, Belgium, GLPS: Puerto Ayora, Galapagos Island, Ecuador, CAS1: Casey, Australian Antarctica Territory, YSSK: Yuzhno-Sakhalinsk, Sakhalin Region, Russia

The receiver clock BRUS (Brussels, Belgium)—steered by a hydrogen maser clock—was used as reference clock. As expected, all three clock correction differences show a different behavior according to their frequency normal.

For validating the clock densifications from 5 min to 5 s it is important that the lines for the different densifications reflect the same solution (red: 5 s, green: 30 s, and blue: 300 s sampling). This is the case for all three examples, implying that an increased sampling from one solution step to the next works as a very good interpolation.

For completeness we include the Allan deviations for two of the GPS satellite clocks (G03 and G29) in Fig. 6. BRUS is again used as reference clock. For satellite clock corrections interpolation from one solution step to the next one works as in the case of the ground based clocks.

4.2 Kinematic PPP with shifted epochs

In order to validate the quality of the high-rate clocks generated with the EHRI approach we perform a kinematic PPP with shifted observations epochs. First we use the high-rate 30-s clock corrections for a kinematic PPP with a nominal 5-min sampling (0, 5 min, etc.), which is independent of the generation of high-rate clock corrections. The 5-min clock corrections are generated with the preceding zero-difference network solution. If the observation epochs are shifted by 30 s (0:30, 5:30 min, etc.) we also get kinematic positions with a 5-min sampling, but based on satellite clock values obtained by the interpolation procedure using the phase-difference observations. If the interpolated clock corrections have the same quality as the nominal 5-min clock corrections, the result of the kinematic PPP with the shifted observation epochs must be of the same quality. Nine of these shifted solutions (30, 60, . . . , 270 s) may be generated.

As kinematic positions are estimated epoch-wise for static stations they show variations compared to a static coordinate set estimated for a specific time span. A comparison of the RMS values of these variations may be taken as an indicator of the quality of the kinematic positions.

Figure 7 shows the RMS of these variations for five different stations for the nominal (most left bar for each station) and the nine shifted kinematic PPP solutions. The differences between the ten different kinematic solutions is marginal—no significant degradation can be seen for the solutions with shifted observation epochs. The mean values of the variations (not shown) are also very consistent for the nine solutions for each station. This validation confirms the quality of the high-rate clock corrections obtained by the interpolation algorithm.

5 Validation of reduced sampling rate

One-Hz GPS tracking data for high-accuracy zero-difference applications (e.g., LEO missions like GOCE and MetOp-A, or terrestrial kinematic measurements, airplane positioning) are, or will be available in the near future. Therefore, it is important to know what sampling rate is required for the GPS satellite clock correction in order not to lose precision for 1-s PPP.

As the IGS provides data for a 1-Hz ground station network 1-s GPS satellite clock corrections may be determined using these data. The data amount and the computation time, even for the EHRI algorithm presented in this paper, is very long, however. The computation time for a 1-s solutions is at least 30 times longer than for a 30-s solution because of the epoch-wise processing. Therefore, we studied whether a

reduced sampling is sufficient for the GPS satellite clock corrections to reach the same or an only slightly inferior accuracy as for the full 1-s clock correction set (see also Bock et al. 2007).

The GPS satellite clock correction based on a reduced data set may be validated in two steps:

1. Evaluation of interpolation error for different sampling rates (2, 5, 10, and 30 s).
2. Kinematic point positioning of fixed terrestrial stations using interpolated GPS clock corrections with different sampling rates.

A reference set of 1-s GPS clock corrections is generated for days 140–149 in 2004 based on the EHRI method described in Sect. 3. The clock corrections are fixed to the 30-s CODE final clock corrections. Three additional sets of GPS clock corrections are generated with different spacing (2, 5, and 10 s) based on the same station tracking data set. These clock sets are used for the following investigations together with the 30-s CODE final clocks.

5.1 Evaluation of interpolation errors

One-s clock corrections are derived from n-s ($n > 1$, e.g., $n = 30$ for 30-s clocks) clock corrections by linear interpolation between the n-s values. Then, the differences between the interpolated and the reference 1-s clock corrections are computed. Figure 8 shows the RMS values of these differences for days 141 and 151/2004.

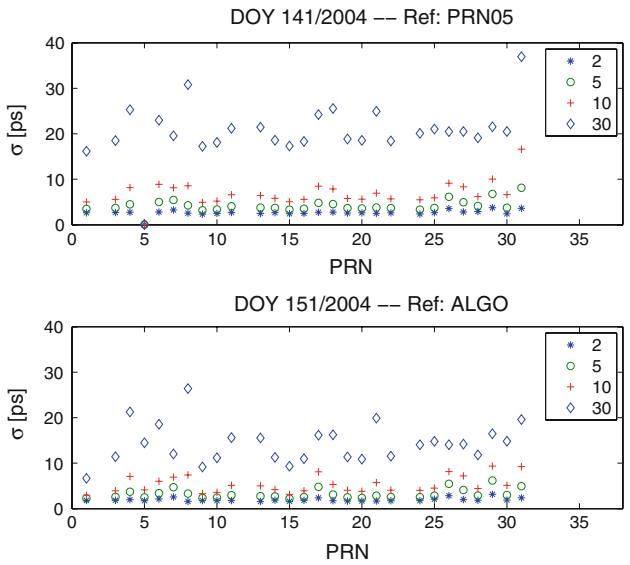

Fig. 8 RMS of differences between 1-s clock corrections and interpolated clock corrections with different spacing (2, 5, 10, and 30 s) for each PRN

The RMS values are given for each of the GPS satellites. The reference clock is that of satellite PRN 5 on day 141 (small RMS values for PRN 5) and the hydrogen maser clock at ALGO on day 151.

Interpolation of clock corrections is affected by a non-linear reference clock. Therefore, a good reference clock should be selected (see Sect. 2.3). The impact of the reference clock shows up in Fig. 8. The RMS values are smaller for day 151/2004, where a Hydrogen maser serves as reference. The clock corrections with the 30-s sampling (all other clock correction sets are fixed to these 30-s values) are also included. The RMS values for the interpolated 30-s clock corrections are of the worst quality with values up to 40 ps. For the sampling of 2 and 5 s all values are well below 10 ps, corresponding to 3 mm.

5.2 Kinematic point positioning of terrestrial station

Two stable stations TASH (Tashkent, Uzbekistan) and TIDB (Tidbinbilla, Australia) providing 1-s GPS tracking data are selected for kinematic point positioning. The five sets of GPS clock corrections are used to generate five kinematic solutions. Due to the linear interpolation of the clock corrections based on n-s data, $n > 1$, we expect to see systematic errors in the coordinates. The differences in the 3-D RMS errors of the kinematic point positions with respect to a static coordinate solution show the impact of these systematic errors on the resulting positions.

Figure 9 shows the deterioration of the 3-D RMS errors resulting from a 1-s kinematic point positioning for TASH (left) and TIDB (right) for ten days (140 to 149/2004) using interpolated GPS clock corrections with different spacing (2, 5, 10, and 30 s) relative to the reference solution with the 1-s clock correction. As expected, the RMS errors grow with increased sampling intervals of the clock corrections. The use of interpolated clock corrections based on a 5- or 2-s sampling is not significantly worse than the use of the reference clock corrections with 1-s sampling. With 2-s clock corrections the deterioration is below 1% and with 5-s clock corrections below 2%. Starting with clock corrections separated by 10 s (up to 6% for station TIDB) the accuracy of the kinematic positions degrades significantly.

Figure 10 shows the differences in the North component between the kinematic solutions (TASH, day 140, 2004) from the GPS clock corrections at different spacings and the reference 1-s clock set. The largest differences can be seen for the solution with interpolated 30-s clock corrections. For the solutions using interpolated 2-s clock corrections the differences are smaller than 0.5 mm and for the 5-s clock corrections the differences are still well below 1 mm for a majority of the epochs. The remaining two solutions show systematic effects introduced by the clock interpolation.

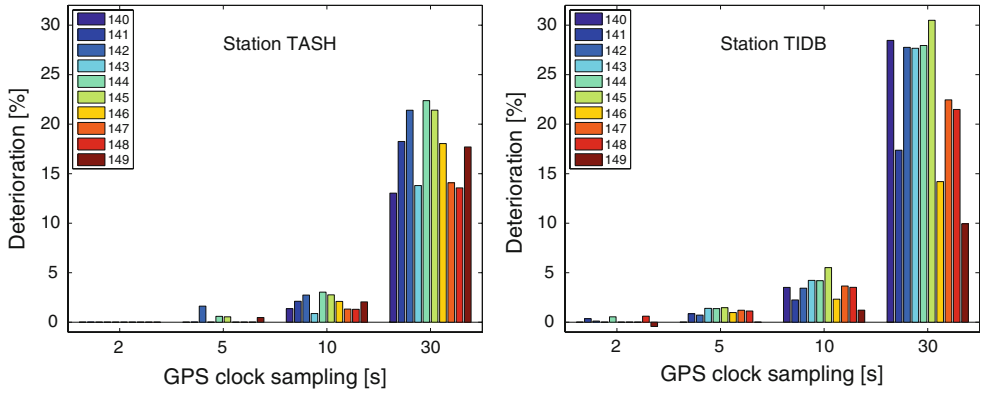

Fig. 9 Deterioration of 3D-RMS error [%] for 1-s kinematic point positioning using different sampled GPS clock corrections (2, 5, 10, and 30 s, relative to 1-s reference solution) for stations TASH (*left*) and TIDB (*right*) for days 140–149, year 2004, not visible bars mean no deterioration (0%)

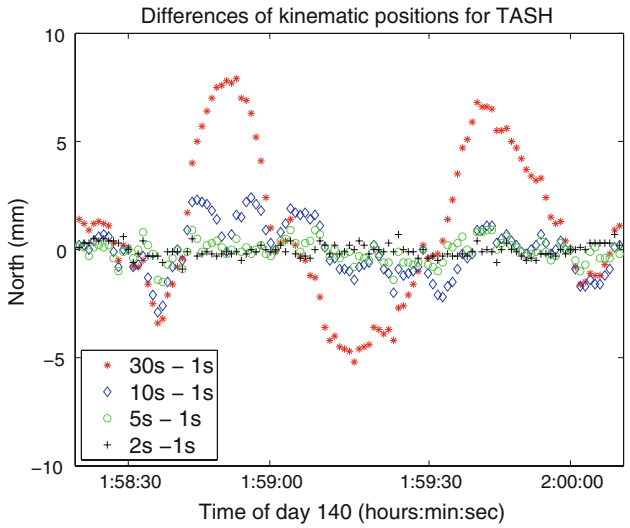

Fig. 10 Station TASH—kinematic point positioning on day 140/2004 using different interpolated and the reference GPS clock corrections, differences (North component) to static coordinate solution

We conclude that the impact on the kinematic positions is marginal when using interpolated 5- or 2-s GPS clock corrections instead of the reference clock set based on the original 1-s sampling.

6 Application: LEO POD for gravity field determination

Precise determination of LEO orbits, which are required for recovering the static part of the Earth's gravity field, is one important application of high-rate GPS clock corrections. For the GOCE mission, e.g., GPS tracking data serve as the primary data source for the determination of the low degree spherical harmonic coefficients, because the measurements of the core instrument, the three-axis gravity gradiometer, are band-limited (Pail et al. 2006). Gravity field groups within the GOCE HPF rely on the precise 1-s kinematic positions computed within the framework of the HPF (Bock et al. 2007). As kinematic positions referring to different epochs are, in essence, independent, every data point contains gravity field information. The dense 1-s sampling of the kinematic positions is thus helpful to significantly reduce the propagation of the positioning errors into the estimated gravity field coefficients (e.g., Jäggi et al. 2008).

GPS tracking data of GRACE-A covering days 100–109 of the year 2007 have been used to illustrate the benefit of high-rate GPS clock corrections for kinematic orbit determination. As GRACE GPS data are available with 10-s sampling only, reduced-dynamic and kinematic solutions based on the full amount of GPS data have been computed by either using 5-s GPS clock corrections (downsampled to 10 s) for both orbit solutions, or by using 30-s GPS clock corrections (linearly interpolated to 10 s) for both orbit solutions. The kinematic positions are computed with a sampling of 10 s for both types of GPS clock corrections.

Figure 11 (top) shows for day 100/2007 the radial differences between the kinematic and the reduced-dynamic

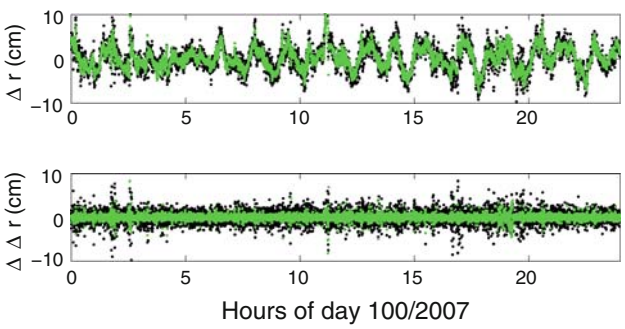

Fig. 11 Radial differences between kinematic and reduced-dynamic positions when using downsampled 5-s GPS clock corrections (green) or the interpolated 30-s clock corrections (black), GRACE A, day 100 of the year 2007

Table 1 Mean RMS (cm) for differences and time differences between kinematic and reduced-dynamic positions, GRACE A, days 100-109 of the year 2007

	R		A		O	
	I	F	I	F	I	F
Differences	2.6	2.3	2.0	1.8	1.9	1.9
Time differences	1.3	0.6	0.6	0.3	0.4	0.2

RAO: radial, along-track, and out-of-plane directions; I: interpolated 30-s clock corrections, F: fixed 5-/10-s clock corrections

positions when using the downsampled 5-s GPS clock corrections or the interpolated 30-s clock corrections. Although a small improvement is also confirmed by Table 1 for the 10-day data set, Fig. 11 (top) primarily reveals systematic differences between kinematic and reduced-dynamic orbits rather than the impact of high-rate GPS clock corrections. In order to avoid these low-frequency effects, which are not related to the discussion in this article, Fig. 11 (bottom) shows time differences of positions for both series. Assuming that reduced-dynamic orbits are significantly less affected by individual measurement errors than kinematic orbits due to the constraints imposed by dynamic models, Fig. 11 (bottom) reveals the high-frequency behavior of the kinematic solutions (corresponding to the left part of an Allan deviations plot). One can see that the kinematic positions are noisier when the interpolated 30-s GPS clock corrections are used instead of the downsampled 5-s clock corrections. Table 1 shows that a degradation of up to a factor 2.2 has to be expected for all components without taking into account the GPS high-rate corrections. This fact is of particular importance for the anticipated gravity field recovery from GOCE kinematic positions.

7 Summary and conclusions

The CODE analysis center at AIUB contributes to the IGS rapid and final clock product with 30- and 5-s clock corrections, respectively. These high-rate clock corrections are determined with an efficient algorithm (EHRI) based on epoch-differenced phase observations. The complete procedure for the rapid and final clock determination at CODE has been described in detail in this article. The 5-min GPS satellite and station clock corrections are determined in a full zero-difference network solution followed by the determination of 30- and 5-s clock corrections based on the special EHRI algorithm. The emphasis has been put on the efficiency of this algorithm. It has been shown that the simplifications made (neglecting of correlations for phase-difference processing) in order to get an efficient algorithm have no significant negative impact on the quality of the resulting high-rate clock corrections.

High-accuracy zero-difference applications based on 1 Hz GPS tracking data require 1-s GPS clock corrections. The generation of 1-s GPS clock corrections is, however, time-consuming even with the EHRI algorithm. It could be shown that GPS high-rate clock corrections with a spacing of 5 s between epochs may be linearly interpolated by users to support 1 Hz applications. A degradation $< 2\%$ was observed when using the 5-s clock corrections instead of 1-s clock corrections for a 1-s kinematic point positioning. The reduction of the sampling rate significantly reduces computation time and storage amount for the data and the clock product. This aspect is important even in our era, where processing power increases significantly as a function of time.

References

Allan D (1987) Time and frequency (time-domain) characterization, estimation, and prediction of precision clocks and oscillators. In: IEEE transactions of ultrasonics, ferroelectrics, and frequency control, vol UFFC–34(6)

Beutler G, Brockmann E, Hugentobler U, Mervart L, Rothacher M, Weber R (1996) Combining consecutive short arcs into long arcs for precise and efficient GPS orbit determination. J Geod 70:287–299

Bock H (2004) Efficient methods for determining precise orbits of low earth orbiters using the Global Positioning System. Geodätisch-geophysikalische Arbeiten in der Schweiz, Band 65, Schweizerische Geodätische Kommission, Institut für Geodäsie und Photogrammetrie, Eidg. Technische Hochschule Zürich, Zürich

Bock H, Beutler G, Schaer S, Springer TA, Rothacher M (2000) Processing aspects related to permanent GPS arrays. Earth Planets Space 52:657–662

Bock H, Hugentobler U, Springer T, Beutler G (2002) Efficient precise orbit determination of LEO satellites using GPS. Adv Space Res 30(2):295–300

Bock H, Jäggi A, Švehla D, Beutler G, Hugentobler U, Visser P (2007) Precise orbit determination for the GOCE satellite using GPS. Adv Space Res 39(10):1638–1647. doi:10.1016/j.asr.2007.02.053

Dach R, Schildknecht T, Hugentobler U, Bernier LG, Dudle G (2006) Continuous geodetic time transfer analysis method. IEEE Trans Ultrason Ferroelectr Freq Control 53(7):1250–1259

Dach R, Hugentobler U, Fridez P, Meindl M (eds) (2007) The Bernese GPS software version 5.0. Astronomical Institute, University of Bern

Dach R, Brockmann E, Schaer S, Beutler G, Meindl M, Prange L, Bock H, Jäggi A, Ostini L (2009) GNSS processing at CODE: status Report. J Geod 83(3–4):353–365. doi:10.1007/s00190-008-0281-2

Dow J, Neilan R, Rizos C (2009) The International GNSS Service in a changing landscape of Global Navigation Satellite Systems. J Geod 83(3–4):191–198. doi:10.1007/s00190-008-0300-3

Drinkwater M, Haagmans R, Muzi D, Popescu A, Floberghagen R, Kern M, Fehringer M (2006) The GOCE gravity mission: ESA's first core explorer. In: Proceedings 3rd GOCE User Workshop, 6–8 November 2006, Frascati, Italy, ESA SP-627, pp 1–7

Gendt G (2006) Combined IGS clocks with 30 second sampling rate. IGS Mail No. 5525, IGS Central Bureau Information System

Gurtner W (1994) RINEX: The receiver-independent exchange format. GPS World 5(7):48–52. Format specifications available at ftp://igscb.jpl.nasa.gov/igscb/data/format/rinex2.txt

Hugentobler U (2004) CODE high rate clocks. IGS Mail No. 4913, IGS Central Bureau Information System

Hwang C, Tseng T, Lin T, Švehla D, Schreiner B (2008) Precise orbit determination for the FORMOSAT-3/COSMIC satellite mission using GPS. J Geod doi:10.1007/s00190-008-0256-3

Jäggi A (2007) Pseudo-stochastic orbit modeling of low Earth satellites using the Global Positioning System. Geodätisch-geophysikalische Arbeiten in der Schweiz, Band 73, Schweizerische Geodätische Kommission, Institut für Geodäsie und Photogrammetrie, Eidg. Technische Hochschule Zürich, Zürich

Jäggi A, Hugentobler U, Beutler G (2006) Pseudo-stochastic orbit modeling techniques for low-Earth orbits. J Geod 80(1):47–60

Jäggi A, Hugentobler U, Bock H, Beutler G (2007) Precise orbit determination for GRACE using undifferenced or doubly differenced GPS data. Adv Space Res 39(10):1612–1619. doi:10.1016/j.asr.2007.03.012

Jäggi A, Bock H, Pail R, Goiginger H (2008) Highly-reduced dynamic orbits and their use for global gravity field recovery: a simulation study for GOCE. Stud Geophys Geod 52(3):341–359

Koop R, Gruber T, Rummel R (2006) The status of the GOCE high-level processing facility. In: Proceedings 3rd GOCE User Workshop, 6-8 November 2006. Frascati, Italy, ESA SP-627, pp 199–205

Kroes R (2006) Precise relative positioning of formation flying spacecraft using GPS. Optima Grafische Communicatie, Rotterdam. ISBN 90-8559-150-3

McCarthy D, Petit G (2004) IERS conventions (2003). IERS Technical Note 32, Bundesamt für Kartographie und Geodäsie, Frankfurt am Main

Montenbruck O, Gill E, Kroes R (2005) Rapid orbit determination of LEO satellites using IGS clock and ephemeris products. GPS Solutions 9:226–235. doi:10.1007/s10291-005-0131-0

Noll C, Bock Y, Habrich H, Moore A (2009) Development of data infrastructure to support scientific analysis for the International GNSS Service. J Geod 83(3–4):309–325. doi:10.1007/s00190-008-0245-6

Pail R, Metzler B, Lackner B, Preimesberger T, Höck E, Schuh WD, Alkathib H, Boxhammer C, Siemes C, Wermuth M (2006) GOCE gravity field analysis in the framework of HPF: operational software system and simulation results. In: Proceedings 3rd GOCE User Workshop, 6-8 November 2006. Frascati, Italy, ESA SP-627, pp 249–256

Press WH, Teukolsky S, Vetterling WT, Flannery BP (1996) Numerical Recipes in Fortran 77. The Art of Scientific Computing, 2nd edn. Cambridge University Press, London

Reigber C, Lühr H, Schwintzer P (2002) CHAMP mission status. Adv Space Res 30(2):129–134

Schaer S (1999) Mapping and predicting the Earth's ionosphere using the Global Positioning System, Geodätisch-geophysikalische Arbeiten in der Schweiz, vol 59. Schweizerische Geodätische Kommission, Institut für Geodäsie und Photogrammetrie, Eidg. Technische Hochschule Zürich, Zürich, Switzerland

Schaer S, Dach R (2008) Model changes made at CODE. IGS Mail No. 5771. IGS Central Bureau Information System

Springer T (2000) Modeling and validating orbits and clocks using the Global Positioning System. Geodätisch-geophysikalische Arbeiten in der Schweiz, Band 60, Schweizerische Geodätische Kommission, Institut für Geodäsie und Photogrammetrie, Eidg. Technische Hochschule Zürich, Zürich

Tapley B, Bettadpur S, Ries J, Watkins M (2004) GRACE measurements of mass variability in the Earth system. Science 305(5683):503–505

Van Helleputte T, Visser P (2008) GPS based orbit determination using accelerometer data. Aerosp Sci Technol 12:478–484. doi:10.1016/j.ast.2007.11.002

Zumberge JF, Heflin MB, Jefferson DC, Watkins MM, Webb FH (1997) Precise point positioning for the efficient and robust analysis of GPS data from large networks. J Geophys Res 102(B3):5005–5017